PHYSICAL REVIEW A VOLUME 26, NUMBER 6 DECEMBER 1982

Distorted-wave electron-impact ionization cross sections for the argon isoelectronic sequence

S. M. Younger
Atomic and Plasma Radiation Division, Center for Radiation Research, National Bureau of Standards, Washington, D.C. 20234
(Received 2 March 1982)

Electron-impact ionization cross sections have been calculated in a distorted-wave exchange approximation for seven ions in the argon isoelectronic sequence. For neutral argon, target configuration interaction and term dependence in the ejected-electron continuum were found to be significant influences on the cross section. Similarities of electron ionization and photoionization are discussed. An analytic fit is given which accurately reproduces the distorted-wave cross sections and rate coefficients of argonlike ions with $Z \geq 20$.

I. INTRODUCTION

Electron-impact ionization cross sections are important components in modeling the structure and dynamics of high-temperature plasmas occurring both naturally in stars and artificially in fusion plasma devices. Although a significant amount of new information concerning the electron ionization of highly charged ions has become available in the past few years,[1-3] most of this data has concerned relatively light target ions with from one to eleven electrons. Very recent theoretical[4] and experimental[5] work on several-times-ionized transition-group elements has concentrated on mapping out the complex resonance structures embedded in the ejected-electron continuum, but very little information is available concerning the direct ionization process for many-electron ions.

The argon sequence is a practical choice for such a study for several reasons. First, having a closed-shell ground state, the atomic structure of argonlike ions is relatively simple, and dominant correlation contributions to the wave function can be represented in a reasonably compact fashion. Second, the complex resonance structures in the ejected-electron continuum which dominate the shape of the cross section for many heavy ions are very weak in argonlike ions, since the first autoionizing states are of the type $3s\,3p^6nl$, which have relatively small excitation cross sections compared to the direct ionization process. Third, there is available an extensive series of calculations of the photoionization cross sections of argonlike ions which can serve as guides in understanding the behavior of the slow ejected electron in electron ionization.

Section II briefly describes the distorted-wave method employed in the present work. Section III describes the calculations for neutral argon with special attention given the importance of initial- and final-state electron correlation in the calculation of an accurate electron ionization cross section. Section IV presents results for the argonlike ions K II, Ca III, Sc IV, V VI, Fe IX, and Kr XIX. Section V concludes the paper.

II. COMPUTATIONAL METHOD

The distorted-wave Born-exchange approximation employed here has been described in detail elsewhere.[1] Briefly, a triple partial-wave expansion describes the incident, scattered, and ejected electrons. The incident and scattered waves are computed in the potential of the target ground state. The low-energy final-state (ejected) wave is computed in the potential of the ion. The potentials consist of the static electrostatic potentials of the nucleus and bound target electrons plus a semiclassical exchange (SCE) potential[6] which has been found to accurately approximate partial-wave orbitals computed in a frozen-core configuration-averaged Hartree-Fock nonlocal exchange potential. For the target orbitals we used the analytic Hartree-Fock wave functions of Clementi and Roetti.[7] For ejection of a $3p$ electron the maximum incident, scattered, and ejected partial-wave orbital angular momenta considered were 14, 14, and 8, respectively. For $3s$-electron ejection the corresponding maximum partial-wave momenta considered were 10, 10, and 6 for incident energies less than twice the ionization energy and 14, 14, and 10 for higher incident energies. These limits were found adequate to ensure convergence of the partial-wave expansions to within a few percent. The residual contribution was included by simple

extrapolation of partial cross sections.

The cross sections were computed in the maximum interference approximation of Peterkop,[8] which maximizes the effect of scattering exchange in the final two-continuum electron state and hence minimizes the total ionization cross section. While there is no *a priori* justification for this choice over other possible final-state phase conventions, the maximum interference approximation has been found to yield theoretical cross sections in good agreement with available experimental data for a variety of atoms and ions.[1] Typically, the Born-exchange cross section exceeds the Born value at low incident electron energies. At $u=1.25$ the increase amounts to 10–20%, being smaller for higher stages of ionization. Here u is the incident electron's energy in units of the $3p$ ionization energy. As the incident electron energy increases, the exchange cross section decreases relative to the direct cross section, becoming smaller for $u \gtrsim 2$. At $u=5$ the exchange values are about 10% below the direct.

Experimental ionization energies were used where they were available and are listed in Table I.

III. ARGON

A number of measurements of the electron-impact ionization cross section of neutral argon have been performed; a critical review of the available data may be found in a paper by Kieffer and Dunn.[9] We have chosen the results of Asundi and Kurepa[10] for comparison purposes since they are representative of the majority of the measurements. As Kieffer and Dunn point out, however, a careful measurement by Rapp and Englander-Golden[11] yielded cross sections about 20–30% lower than those of Asundi and Kurepa and others near the cross-section maximum. They suggest that this figure is an indication of the systematic errors which could affect the experimental data.

Previous calculations of the *photo*ionization cross section of neutral argon have demonstrated the importance of electron correlation in both the initial and final states in determining an accurate total cross section.[12,13] We expect a similar situation to prevail in the case of electron ionization. Since the distorted-wave theory employed here ignores interactions between the target and the incident and scattered waves beyond the atomic potential in which the partial waves are calculated, the electron ionization process is essentially portrayed by this theory as a one-electron excitation propagated by a "transition potential" due to the scattering electron. We have found in the past that the total electron ionization cross section is much less sensitive to the details of the incident-scattered partial-wave potential than to the choice of the potential for the ejected wave. Thus the most important improvements in the simple distorted-wave theory outlined above are expected to occur in the description of the initial and final target states, the later representing the ejected continuum electron. Unless otherwise noted, all of the calculations discussed below were made with incident and scattered partial waves computed in a semiclassical exchange potential.

The results of our calculations are shown in Fig. 1. The lowest-order approximation which we ap-

TABLE I. Ionization energies of argonlike ions (eV).

Ion	I_{3p}	I_{3s}
Ar I	15.76	29.20
K II	31.63	47.76
Ca III	50.91	69.71
Sc IV	73.49	94.93
V VI	128.1	155.0
Fe IX	233.6	268.2
Kr XIX	785	856

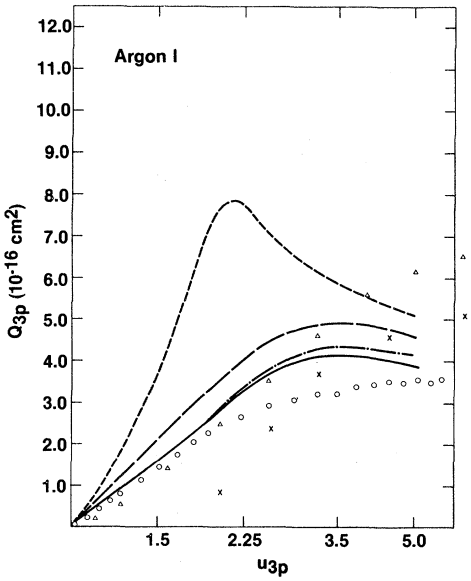

FIG. 1. Electron-impact ionization cross section of neutral argon. ----, distorted-wave exchange, SCE orbitals; — — —, distorted-wave exchange with TDHF ejected d waves; ——, distorted-wave exchange, TDHF d waves, with approximate ground-state correlation; —·—, solid curve plus cross section for ionization of $3s$ subshell; ○, experiment, Ref. 10; ×, plane-wave Born, Ref. 17; △, plane-wave Born, Ref. 16.

plied used a single-configuration Hartree-Fock target wave function and ejected partial waves computed in the configuration-averaged semiclassical exchange potential described in Sec. II. The total cross section resulting from this approximation is in very poor agreement with experiment[10] and exhibits a sharp downturn at about $u=2.0$, where u is the reduced incident electron energy measured in units of the $3p$ ionization energy. Examination of the distribution of the cross section versus the ejected partial-wave angular momentum reveals it to be dominated by the $3p$-Kd dipole transition, which constitutes more than 75% of the total cross section throughout the incident electron energy range considered. This is in contrast to the results of many other calculations of electron ionization cross sections which we have performed, where the

$$nl \rightarrow K(l+1)$$

ejected-electron channel seldom dominates the cross section at low incident electron energies and is often less important than nearby nondipole channels.

The $3p^5Kd$ configuration has three terms ^3P, ^3D, and ^1P corresponding to different couplings of the $3p$ and Kd orbitals. In the first Born approximation, only the $3p^5Kd\ ^1P$ term contributes to the direct matrix element. The triplet terms appear only in the exchange matrix elements. In order to improve the description of the Kd ejected wave, we replaced the semiclassical exchange potential for the Kd ejected wave by the frozen-core term-dependent Hartree-Fock (TDHF) potential for the $3p^5KD\ ^1P$ channel which is given by[14]

$$V_{\mathrm{TDHF}}P(Kd;r)=\left[-\frac{Z}{r}+\sum_{i=1}^{N}J_i(r)\right]P(Kd;r)-X(r)-\left(\tfrac{1}{5}J_{3p}+\tfrac{19}{15}K^1_{3p}-\tfrac{3}{70}K^3_{3p}\right)P(Kd;r)\ , \tag{1}$$

where Z is the nuclear charge, N the number of target electrons, and $X(r)$ is the configuration-averaged nonlocal Hartree-Fock exchange potential.[14] The direct and exchange potential operators are

$$J_i=\frac{1}{r}\int_0^r |P_i(\rho)|^2 d\rho+\int_r^\infty \frac{|P_i(\rho)|^2}{\rho}d\rho \tag{2}$$

and

$$K_i^\lambda P(Kd;r)=\left[\frac{1}{r^{\lambda+1}}\int_0^r P_i(\rho)\rho^\lambda P(Kd;r)d\rho+r^\lambda\int_r^\infty \frac{P_i(\rho)P(Kd;r)}{\rho^{\lambda+1}}d\rho\right]P_i(r)\ , \tag{3}$$

respectively.

$P_i(r)$ is the ith bound radial orbital and $P(Kd;r)$ is the continuum radial orbital. Hartree-Fock ground-state orbitals for neutral argon were used to construct V_{TDHF}. Note that V_{TDHF} is a nonlocal energy-dependent potential. V_{TDHF} differs significantly from the semiclassical exchange potential approximation in that for neutral argon it is effectively a double-well potential. The strong exchange interaction between the Kd ejected wave and the $3p^5$ core, when combined with the attractive nuclear potential and the repulsive potentials due to the direct electrostatic electron interaction and the centrifugal term $l(l+1)/r^2$ in the Hamiltonian, yield a deep inner potential well near the nucleus, a potential barrier in the vicinity of the $3p$ subshell, and a very shallow and extended outer well. Low-energy ejected partial waves will not penetrate the barrier and will reside in the outer well with small overlap with the $3p$ subshell. At higher ejected-electron energies the partial waves will penetrate the potential barrier and have a larger overlap with the $3p$ subshell. Figure 2 compares the phase shifts δ for Kd partial waves computed in the semiclassical exchange potential and the term-dependent Hartree-Fock potential. Whereas δ_{SCE} is large even at low continuum energies, δ_{TDHF} is very small until approximately 0.3 Ry, where a rapid increase occurs. Presumably, this is where the Kd wave begins to penetrate the potential barrier. As a check, we have used our ejected d-wave orbitals to compute the $3p$ photoionization cross section of Ar I with essentially the same results as Swanson and Armstrong[12] who use a similar method. A detailed discussion of the photoionization cross section's dependence on partial-wave potentials and target atom correlation is given in Refs. 12 and 13.

Term dependence is not included in our calculations of the ejected-electron continuum orbital for partial waves with $l\neq 2$, although it is present in the configuration p^5kl for all nonzero l. Term-dependent effects on the ejected partial waves

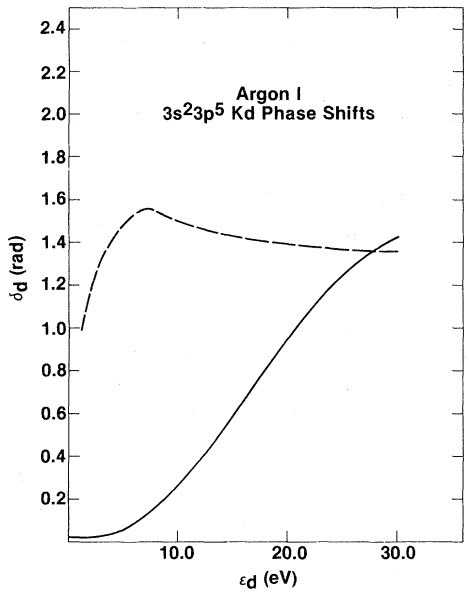

FIG. 2. Ejected d-wave phase shifts for neutral argon. ———, SCE approximation; ——, TDHF approximation.

should decrease rapidly with increasing partial angular momentum due to the increase of the centrifugal term $l(l+1)/r^2$ in the wave equation. At low ejected-electron energies, where the energy-differential cross section peaks, we found only small phase shifts for $l \geq 3$, indicating that further improvement of the potential by including nonlocal term-dependent corrections should be small. Since we have included term dependence in the *Kd* channel, and since it does not exist in the *Ks* channel, the only remaining channel where it is important but not included is the *Kp* channel, which does not play a determining role in the composition of the total cross section. Thus the most significant improvement in the SCE total cross section due to consideration of the term dependence of the ejected continuum wave is expected to ocur in the $3p^5Kd$ channel.

When TDHF *Kd* waves are used to represent the ejected electron, the resulting ionization cross sections are much smaller than when SCE partial waves are used, as is illustrated in Fig. 1. At low incident electron energies the 3*p*-*Kd* partial cross section is reduced by more than a factor of 2 compared to the SCE approximation. At $u=5$ the effect of term dependence is smaller, reducing the SCE result by only about 20%. Also, the sharp downturn in the cross section is absent when TDHF *Kd* waves are used. Again, the curve labeled "TDHF" in Fig. 1 differs from the SCE approximation only in the description of the *Kd* ejected wave. Ejected waves with $l \neq 2$ were computed in the SCE potential. Also, the Kd_{TDHF} partial cross section does not include consideration of scattering exchange. The Born-exchange method demands that the exchange matrix element be constructed from scattered partial waves computed in the potential used for the ejected wave in the direct matrix element.[15] Because of the substantial difference between the SCE scattered electron potential and the TDHF ejected-electron potential, it seems that the Born-exchange approximation would have little physical meaning in this case. Partial cross sections for $l_{\mathrm{ejected}} \neq 2$ do include scattering exchange. Agreement with experiment is improved when TDHF *Kd* partial waves are employed, but is still not satisfactory owing to the neglect of scattering exchange in the *Kd* ejected partial cross section and the single-configuration approximation for the initial target wave function.

To include a multiconfiguration expansion for the initial target state in a partial-wave ionization theory would be a considerable task, owing to the very large number of matrix elements to be computed in a triple partial-wave expansion and the coherent addition of matrix elements in the scattering amplitude arising from the component configurations.

In order to estimate the magnitude of initial target state correlation corrections to the total electron ionization cross section, we have therefore adopted a simpler, more approximate approach: We computed single- and multi-target-configuration ionization cross sections in the simple plane-wave Born approximation, took the ratio of the two, and multiplied the TDHF distorted-wave cross section by this ratio to obtain an approximate correction for ground-state correlation.

In the multiconfiguration plane-wave approximation, the initial target ground state was represented by the four-term expansion

$$\Psi[3p^6\,{}^1S] = c_1\Phi[3p^6\,{}^1S] + c_2\Phi[3p^4({}^1S)3d^2\,{}^1S] + c_3\Phi[3p^4({}^3P)3d^2\,{}^1S] + c_4\Phi[3p^4({}^1D)3d^2\,{}^1S]\,, \tag{4}$$

where Ψ is the correlated wave function, c_i are mixing coefficients, and Φ are component configurations. For our approximate calculations a 3*d* correlation orbital was computed in the static (no-exchange) potential of the $3s^23p^4$ configuration. Ground-state neutral argon bound orbitals were used throughout the calculations. The mixing coefficients which were obtained by means of first-order perturbation theory were $c_1 = 0.9753$,

$c_2=-0.1076$, $c_3=-0.1547$, and $c_4=-0.1151$. While approximate, these choices should represent the dominant ground-state correlation in neutral argon.

The scattering amplitude in the plane-wave Born approximation is given by

$$f_K=\frac{1}{2\pi}\int\int \Psi(3p^6\,{}^1S)\frac{\exp[i(\vec{\mathrm{K}}_i-\vec{\mathrm{K}}_f)\cdot\vec{\mathrm{r}}_2]}{r_{12}}\Psi(3p^5Kl)d\vec{\mathrm{r}}_1 d\vec{\mathrm{r}}_2\ , \tag{5}$$

where $\vec{\mathrm{K}}_i$ and $\vec{\mathrm{K}}_f$ are the incident and final momentum vectors of the scattered electron and K is the momentum of the ejected electron. When the Neumann expansion for the exponential is inserted into Eq. (5), one evaluates matrix elements of the type

$$\langle \Psi(3p^6\,{}^1S)\,|\,j_l(\mathrm{Kr})\,|\,\Psi(3p^5Kl)\rangle\ ,$$

where j_l is the lth-order spherical Bessel function. The first term of the correlation expansion [Eq. (4)] yields the single-configuration matrix element multiplied by the mixing coefficient c_1. The remaining contributions are of the form

$$\langle \Phi[3p^4({}^SL)3d^2\,{}^1S]\,|\,j_l(\mathrm{Kr})\,|\,\Psi[3p^5Kl]\rangle \sim\langle 3d\,|\,Kl\rangle\langle 3d\,|\,j_l(\mathrm{Kr})\,|\,3p\rangle\ , \tag{6}$$

i.e., an excitation-type scattering matrix element times an overlap integral involving the $3d$ correlation orbital and the ejected continuum wave. Since partial waves with different l are orthogonal, ground-state correlation affects only the ejected d waves. Note that the $3d$ correlation orbital was purposely chosen to have a large overlap with the $3p$ subshell for efficient correlation purposes, so the excitation matrix element will be large. Since the correlation orbital and the $Kd\ {}^1P$ ejected wave are computed in different potentials, they will not necessarily be orthogonal. At low ejected-electron energies $\langle 3d\,|\,Kd\rangle$ is approximately unity. As the ejected-electron energy increases, the overlap decreases, falling to ~ 0.17 at $K^2=2.2$ Ry. In argon-like *ions* $\langle 3d\,|\,Kd\rangle$ is much smaller than in neutral argon, since the potential due to the excess nuclear charge overwhelms the exchange potential in V_{TDHF}, resulting in stronger orthogonality between the $3d$ correlation orbital and the ejected d waves.

Table II is a comparison of the results of the various approximations employed. Ground-state correlation reduces the single-configuration $3p$-Kd TDHF cross section by almost a factor of two at $u=1.50$. At higher incident energies the reduction is smaller, mainly due to the smaller overlap of the $3d$ and Kd orbitals for the higher ejected-electron energies involved. Since the cross section for electron ionization is heavily weighted toward low ejected-electron energies, however, correlation effects are expected to remain significant until fairly high incident electron energies. The results of the approximate correlation calculation are seen in Fig. 1 to be in reasonably good agreement with available experimental data. Note the large difference between the plane-wave Born cross sections of Refs. 16 and 17. This difference is due mainly to the use of different ejected partial waves by the two authors: Peach[16] using $Z=1$ regular Coulomb waves and McGuire[17] using distorted waves generated in

TABLE II. Comparison of different approximations for the $3p$-subshell electron ionization cross section of neutral argon (10^{-16} cm^2).

u_{3p}	$Q_{\mathrm{Total}}^{\mathrm{SCE}}$	Q_d^{SCE}	Q_d^{TDHF}	Q_d^{BTDHF}	Q_d^{BTDHFCI}	$\frac{Q^{\mathrm{BTDHFCI}}}{Q^{\mathrm{BTDHF}}}$	Q_d^{TDHFCI}	$Q_{\mathrm{Total}}^{\mathrm{TDHFCI}}$
1.5	3.80	2.96	1.28	0.437	0.255	0.583	0.746	1.59
2.25	7.72	6.13	2.47	1.56	1.09	0.696	1.72	3.31
3.5	5.88	4.47	3.52	3.06	2.35	0.765	2.69	4.10
5.0	5.11	3.74	3.24	3.46	2.69	0.778	2.52	3.89

$Q_{\mathrm{Total}}^{\mathrm{SCE}}$: Distorted-wave Born exchange with SCE scattering waves and SCE ejected waves.
Q_d^{SCE}: Ejected d-wave contribution to $Q_{\mathrm{Total}}^{\mathrm{SCE}}$.
Q_d^{TDHF}: Ejected d-wave cross section, SCE scattering waves, TDHF ejected waves.
Q_d^{BTDHF}: Ejected d-wave cross section, plane-wave scattering waves, TDHF ejected waves.
Q_d^{BTDHFCI}: Q_d^{BTDHF} with ground-state correlation.
Q_d^{TDHFCI}: $Q_d^{\mathrm{TDHF}}\times(Q_d^{\mathrm{BTDHFCI}}/Q_d^{\mathrm{BTDHF}})$.
$Q_{\mathrm{Total}}^{\mathrm{TDHFCI}}$: $Q_{\mathrm{Total}}^{\mathrm{SCE}}$ with Q_d^{TDHFCI} used for the ejected d-wave cross section.

an approximation to the Hartree-Fock-Slater local potential. Our plane-wave Born cross sections are in approximate agreement with those of McGuire,[17] although quite different distorted-wave potentials were employed.

All of the plane-wave Born (PWB) calculations are in very poor agreement with the full distorted-wave calculations, indicating that in neutral argon the approximation for the scattering orbitals is important in the calculation of an accurate total electron ionization cross section. This point will be further discussed in Sec. V. The large difference between the plane-wave and distorted-wave results calls into question the ability of the simple ratio method employed here to give even an approximate idea of initial target state electron correlation effects on the total ionization cross section. Although the ratio method does predict a *decrease* in the single-configuration cross section rather than an increase and does yield reasonable predictions for the magnitude of the correction, it can only be regarded as an approximate indication of the general magnitude of target electron correlation effects. The utility of the simple ratio method described above should thus be viewed in context with the other approximations inherent in the distorted-wave method, such as the neglect of target polarization by the scattering states and the omission of postcollision interaction between the final-state continuum electrons.

IV. ARGONLIKE IONS

Distorted-wave Born-exchange cross sections for the electron ionization of the argonlike ions K II, Ca III, S IV, V VI, Fe IX, and Kr XIX for incident electron energies up to five times threshold are given in Table III. For these cases a single-configuration, SCE distorted-wave potential approximation was employed.

Potassium II is the only positive ion in the argon isoelectronic sequence for which experimental electron ionization data are currently available. Figure 3 compares the results of our distorted-wave Born-exchange calculation using partial waves computed in the SCE approximation to the crossed-beam measurements of Hooper *et al.*[18] and Peart and Dolder.[19] The agreement with experiment is poor at low incident electron energies, although there is a considerable improvement over the situation found in argon. The K^+ theoretical cross section demonstrates the same rapid rise near threshold as was found in the neutral argon SCE calculation, although the effect is less pronounced in potassium. Figure 4 is a Bethe plot of the scaled cross section uI^2Q for several argonlike ions. All of the curves in Fig. 4 were computed using SCE approximation partial waves. The sharp bend in the neutral argon cross section is clearly visible in Fig. 4, as is a similar but smaller bend in the K^+ curve at a somewhat lower reduced incident electron energy. In Ca^{2+}

TABLE III. Scaled electron-impact ionization cross sections uI^2Q for argonlike ions (10^{-14} cm^2 eV^2).

			$3s^23p^6 \rightarrow 3s^23p^5 + e^-$				
u_{3p}	Ar I	K II	Ca III	Sc IV	V VI	Fe IX	Kr XIX
1.25		9.18	4.63	4.18	5.16	6.104	7.08
1.50	5.92[a]	13.0	7.76	7.83	9.46	10.8	12.3
2.25	18.5[a]	17.3	15.4	1.68	19.3	21.0	22.8
3.5	35.6[a]	24.3	24.6	2.70	30.0	31.8	33.1
5.0	48.3[a]	30.8	31.8	34.8	38.3	40.0	40.4
			$3s^23p^6 \rightarrow 3s\,3p^6 + e^-$				
u_{3s}	Ar I	K II	Ca III	Sc IV	V VI	Fe IX	Kr XIX
1.25	1.04	1.87	1.31	1.33	1.61	1.86	2.05
1.50	3.17	2.74	2.21	2.49	2.94	3.29	3.52
2.25	5.92	4.23	4.35	5.22	5.85	6.23	6.37
3.5	8.53	6.96	6.81	8.13	8.86	9.17	9.31
5.0	10.5	7.85	8.67	10.3	11.1	11.4	11.7

[a]Computed with term-dependent Hartree-Fock ejected d waves, with approximate ground-state correlation corrections.

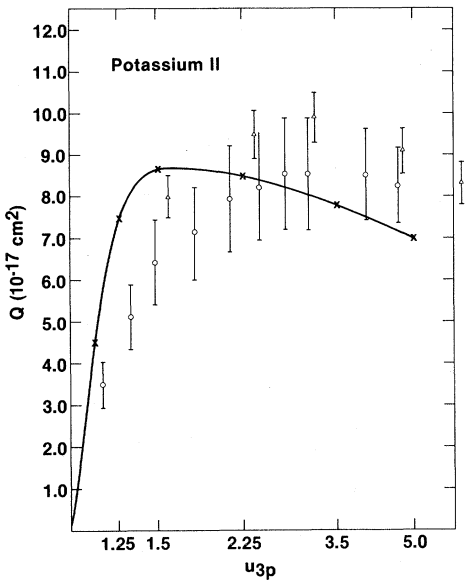

FIG. 3. Electron-impact ionization cross section of potassium II. ——, distorted-wave exchange, SCE orbitals; ○, crossed-beam experiment, Ref. 18; △ crossed-beam experiment, Ref. 19.

one notes only a small effect very near threshold. Beginning at Sc IV the scaled cross section is smoothly varying with both incident electron energy and target nuclear charge. The origin of the abrupt bend in the distorted-wave SCE results for Ar, K^+, and Ca^{2+} is not clear, but is suspected to be an artifact of the SCE potential approximation for the ejected orbitals since it is not present in either the distorted-wave or the plane-wave Born results for Ar I when TDHF ejected orbitals are employed. In both Ar I and K II the total cross section for ionization is dominated by the $3p$-Kd ejection channel, where the effects of ejected term-dependent potentials are most important. The Kd ejected wave does not dominate the total cross section for the highly charged argonlike ions, contributing a smaller fraction of the total as the nuclear charge is increased. Figure 5 illustrates the relative contribution of various ejected waves for K II and V VI versus the incident electron energy. For V VI the $3p$-Kd dipole channel contributes a relatively small part of the total electron ionization cross section for $u < 2$, although its shape indicates a larger relative contribution at higher energies. At very large u the Born limit will be approached with only the Ks and Kd waves contributing substantially.

We have not attempted to include correlation effects in the calculations for the argonlike ions. Preliminary calculations for K II, including term dependence in the ejected channel, indicate an *increase* over the SCE cross section, which may or may not be completely canceled by ground-state correlation. A more sophisticated version of the distorted-wave method is under development which will allow detailed studies of target and ejected-

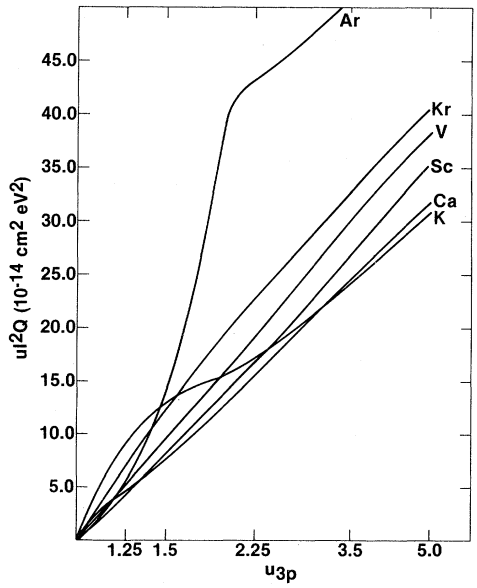

FIG. 4. Bethe plot of the scaled electron ionization cross section uI^2Q for argonlike ions.

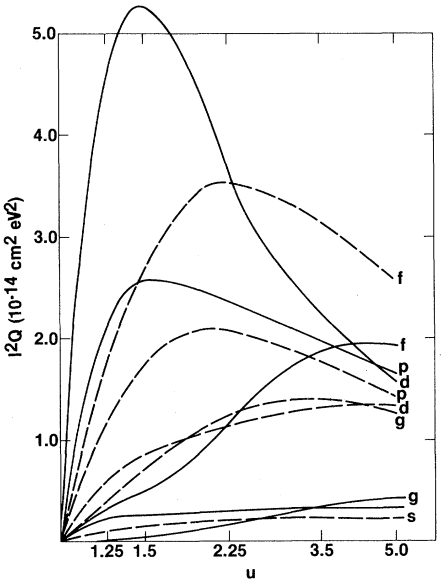

FIG. 5. Partial cross sections for ionization of $3p$ electrons in K II and V VI versus incident electron energy. ——, K II; — — —, V VI. The letters refer to the angular momentum of the ejected partial wave.

electron correlation effects for ions. Since both the ejected-electron continuum term dependence and the overlap integral governing the influence of ground-state correlation on the scattering matrix element both decrease rapidly with increasing Z, we expect the present results to remain relatively unchanged by these effects for $Z > 20$.

In order to illustrate the smooth scaling of the $3p$ ionization cross section as a function of the nuclear charge, we give in Fig. 6 an isoelectronic plot of the scaled ionization cross section uI^2Q vs $1/(Z-17)$, the effective ionic charge. Each curve in Fig. 6 corresponds to a fixed reduced incident electron energy u. For the $Z=\infty$ asymptotic limit, we have employed the scaled Coulomb-Born results of Moores *et al.*[20] The apparent minimum in the isoelectronic curves at low Z is a result of the poor performance of the SCE potential for low charge states. For Sc IV and higher Z the scaled cross section is monotonically increasing with Z.

Although the above discussion has concentrated on electron ionization from the $3p$ subshell, we have also calculated distorted-wave Born-exchange cross sections for ionization from the $3s$ subshell and tabulate them in Table III. All of the $3s$-subshell cross sections, including those for neutral argon, were computed in a single-configuration distorted-wave Born-exchange approximation with SCE partial-wave potentials. For neutral argon the $3s$ cross section is an order of magnitude lower than the one for $3p$ ionization. As the nuclear charge increases, the M shell becomes more compact, so that

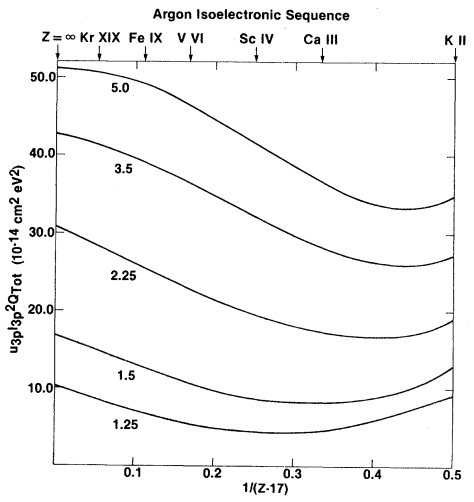

FIG. 6. Isoelectronic plot of the scaled electron ionization cross section uI^2Q for ejection of a $3p$ electron in argonlike ions versus $1/(Z-17)$. Each curve corresponds to a fixed incident electron energy u.

at Kr XIX the $3s$ cross section is 20–25 % of the $3p$ value.

For practical application of the results we have fit the $3p$ and $3s$ cross sections for argonlike ions with $Z \geq 20$ by the formula

$$uI^2Q = A\left[1-\frac{1}{u}\right]+B\left[1-\frac{1}{u}\right]^2 + C\ln u + \frac{D}{u}\ln u \ . \tag{7}$$

The parameter C is a Bethe coefficient describing the slope of the cross section at high incident electron energies and was calculated from the extensive photoionization tabulations of Manson.[21] Parameters A, B, and D were obtained by means of a least-squares fit[22] to the present theoretical data. All of the parameters were then fit by simple expansions in the ionic charge

$$A = \sum_{i=0}^{3} \frac{a_i}{(Z-17)^i}$$
$$B = \sum_{i=0}^{3} \frac{b_i}{(Z-17)^i} \ , \tag{8}$$

etc. The coefficients a_i, b_i, c_i, and d_i are given in Table IV. Electron ionization cross sections may be computed from these formulas for any ion in the argon isoelectronic sequence with $Z \geq 20$ to within a few percent of the results of an actual distorted-wave calculation. Using formulas given in Ref. 22, one may compute the associated electron ionization rate coefficient assuming a Maxwellian electron velocity distribution. Note that the fitting procedures were applied only for $Z \geq 20$, where the ef-

TABLE IV. Isoelectronic parameters describing the electron ionization of highly ionized argonlike ions with $Z \geq 20$ (10^{-14} cm^2 eV^2).

	$3s^23p^6 \rightarrow 3s^23p^5 + e^-$			
	$i=0$	1	2	3
$a_i(3p)$	68.3	222	−2610	7160
$b_i(3p)$	−21.0	−206	2320	−6120
$c_i(3p)$	5.38	74.6	−392	481
$d_i(3p)$	−32.7	−386	2650	−6260
	$3s^23p^6 \rightarrow 3s\,3p^6 + e^-$			
	$i=0$	1	2	3
$a_i(3s)$	23.4	−13.6	−386	1360
$b_i(3s)$	−8.59	−7.32	488	−1500
$c_i(3s)$	2.12	4.87	−33.4	41.4
$d_i(3s)$	−14.7	4.75	230	−912

fects of term dependence in the $3p$ ejected continuum are relatively small and the isoelectronic scaling of the cross section is smooth.

V. DISCUSSION

We have reported the results of distorted-wave Born-exchange calculations of the electron ionization cross sections of seven argonlike ions. For the positive ions and for the $3s$ subshell of neutral argon we employed a single-configuration target state wave function and a local semiclassical exchange potential for the calculation of the partial waves. For ionization from the $3p$ subshell of neutral argon we calculated Kd ejected partial waves in a nonlocal term-dependent Hartree-Fock potential and approximated the effect of ground-state electron correlation on the cross section.

In neutral argon the complex interrelation of correlation in the initial target state and term dependence in the ejected wave was found to radically change the theoretical cross sections from those obtained from a simple static potential distorted-wave approximation. The strong potential-exchange interaction between the $3p^5$ subshell and the $Kd\ ^1P$ ejected partial wave not only reduced the ionization cross section, but also allowed the ground-state pair correlation $3p^6$-$3p^4 3d^2$ to affect the scattering amplitude by means of the large overlap between the $3d$ correlation orbital and the Kd ejected orbital. Without the large term dependence of the ejected continuum the influence of ground-state correlation would have been much weaker, as we found in an earlier calculation for the beryllium isoelectronic sequence.[1]

Ejected waves in argonlike ions more than once or twice ionized will be much less influenced by the $3p$-$Kd\ ^1P$ exchange interactions. Thus one would not expect significant changes in the total electron ionization cross section due to the combination of Kd term dependence plus ground-state correlation for highly charged argonlike ions. The only influence of the $3p^6$-$3p^4 3d^2$ correlation would be in the different matrix elements associated with the $3p$ and $3d$ orbitals, a difference which is expected to be small, as it was in calculations for the analogous $2s^2$-$2p^2$ substitution in berylliumlike ions. Similar conclusions for the photoionization of noble gas isoelectronic sequences have been presented by Msezane *et al.*[23] For the argon sequence, they found that cross sections for $Z \geq 21$ computed in the term-dependent Hartree-Fock approximation with target correlation were in almost exact agreement with results generated in a simple static central potential.

Calculations performed on neutral argon in the distorted-wave and plane-wave Born approximations, using the same approximation for the target and ejected electron wave functions, demonstrate that the cross section is very sensitive to the description of the scattered states, especially at low incident electron energies. This is in contrast to the results of distorted-wave calculations for light neutral atoms such as H and He, where plane-wave Born and distorted-wave results are quite similar. In light atoms, however, there are substantial partial-wave phase shifts only for s and p waves. For heavier atoms such as argon one finds nontrivial phase shifts for much higher partial waves, reflecting increased interaction of the scattering electron with the target. Thus for heavier atoms a larger proportion of the cross section is influenced by the deviation of the scattering approximation from the plane-wave case. For positive ions where the Coulomb potential dominates the partial waves, the total cross section is expected to be much less sensitive to the details of the scattered waves. This last point has been recently discussed by Bottcher.[24]

The sensitivity of the neutral argon cross section to the scattering approximation suggests that one should also consider postcollision interaction of the two final-state continuum waves—omitted in the Born-exchange scattering approximation—if an accurate *ab initio* description of argon ionization is desired. Interactions of three bodies propagated by a Coulomb interaction are beyond the scope of any simple distorted-wave theory, however, being an inherently many-body effect. The present approximation for the scattering orbitals, i.e., a static Hartree-Fock potential plus a semiclassical exchange potential, also does not account for the relaxation of the target wave function under the influence of the scattering waves and as such represents an approximate zeroth-order representation of the electron-target interaction. Since the Born-exchange approximation requires that the incident and scattered orbitals be computed in the same potential, however, such initial-state relaxation effects occupy an analogous position in the theory to postcollision interaction effects in the final state. The frozen-core potential employed in the present work might then be viewed as a somewhat arbitrary compromise between accurate potentials for the initial and the final scattering states. Rather than a rigorous calculation, which is not possible in a strictly distorted-wave approximation, the present results for neutral argon should be regarded as a

demonstration of the kinds of interactions which must be included in a more elaborate study of electron ionization from heavy neutral atoms. This consideration will also apply to a lesser degree to the first few ionization stages of heavy ions. For more highly charged positive ions the present approximation should become more accurate, although more experimental comparisons are required before this is certain.

ACKNOWLEDGMENT

This work was partially supported by the Department of Energy.

[1]S. M. Younger, Phys. Rev. A 22, 111 (1980); 22, 1425 (1980); 23, 1138 (1981); 24, 1272 (1981); 24, 1278 (1981).

[2]H. Jakubowicz and D. L. Moores, Comments At. Mol. Phys. 9, 55 (1980), and references therein.

[3]M. Blaha and J. Davis, Naval Research Laboratory Memorandum Report No. 4245 (unpublished).

[4]D. C. Griffin, C. Bottcher, and M. B. Pindzola (unpublished).

[5]R. A. Falk, G. H. Dunn, D. C. Griffin, C. Bottcher, D. C. Gregory, and D. H. Crandall, Phys. Rev. Lett. 47, 494 (1981).

[6]M. E. Riley and D. G. Truhlar, J. Chem. Phys. 63, 2181 (1975).

[7]E. Clementi and C. Roetti, At. Data Nucl. Data Tables 14, 177 (1974).

[8]R. K. Peterkop, Zh. Eksp. Teor. Fiz. 41, 1938 (1961) [Sov. Phys.—JETP 14, 1377 (1962)].

[9]L. J. Kieffer and G. H. Dunn, Rev. Mod. Phys. 38, 1 (1966).

[10]R. K. Asuni and M. V. Kurepa, J. Electron. Control 15, 41 (1963).

[11]D. Rapp and P. Englander-Golden, J. Chem. Phys. 43, 1464 (1965).

[12]J. R. Swanson and L. Armstrong, Jr., Phys. Rev. A 15, 661 (1977).

[13]H. P. Kelly and R. L. Simmons, Phys. Rev. Lett. 30, 529 (1973).

[14]J. Slater, *Quantum Theory of Atomic Structure* (McGraw-Hill, New York, 1960), Vol. II.

[15]M. R. H. Rudge and M. J. Seaton, Proc. Phys. Soc. London 88, 579 (1966).

[16]G. Peach, J. Phys. B 1, 1088 (1968).

[17]E. J. McGuire, Phys. Rev. A 3, 267 (1971).

[18]J. W. Hooper, W. C. Lineberger, and F. M. Bacon, Phys. Rev. 141, 165 (1966).

[19]B. Peart and K. T. Dolder, J. Phys. B 1, 240 (1968).

[20]D. L. Moores, L. B. Golden, and D. H. Sampson, J. Phys. B 13, 385 (1980).

[21]S. T. Manson (private communication).

[22]S. M. Younger, J. Quant. Spectrosc. Radiat. Transfer 25, 329 (1981).

[23]A. Msezane, R. F. Reilman, S. T. Manson, J. R. Swanson, and L. Armstrong, Jr., Phys. Rev. A 15, 668 (1977).

[24]C. Bottcher (unpublished).